A MEASUREMENT OF pp SPIN CORRELATION COEFFICIENTS AT $6° \leq \theta_{cm} \leq 90°$ BETWEEN 200 AND 450 MeV

B. von Przewoski, W.A. Dezarn, J. Doskow, M. Dzemidzic,
J.G. Hardie, H.O. Meyer, R.E. Pollock, T. Rinckel, and F. Sperisen
Indiana University Cyclotron Facility, Bloomington, Indiana 47408

W. Haeberli, B. Lorentz, F. Rathmann, and T. Wise
University of Wisconsin-Madison, Madison, Wisconsin 53706

P.V. Pancella
Western Michigan University, Kalamazoo, Michigan 49008

Data taking for CE42 was completed in February 1996. The experiment utilized the Wisconsin/IUCF polarized target[1] which has been used by CE35 to measure spin correlation coefficients in pp elastic scattering at 200 MeV at angles $10° \leq \theta_{cm} \leq 35°$ [Ref. 2].

The target cell and detector system are shown in Fig. 1. For ease of tuning and to be less susceptible to shifts in beam position during either the up or the down ramp, which in turn could cause background due to scattering off the cell walls, the cell opening was increased from 8×8 mm^2 (CE35) to 10×10 mm^2. Even though the increased cell diameter causes the target to be thinner by approximately a factor of two, the decrease in time-averaged luminosity is only a few percent, because the ring acceptance (which is determined by the target cell) has been increased. This behaviour has been expected from the results of a dedicated experiment to inverstigate the interplay between cell size, target thickness, ring acceptance and luminosity.[3]

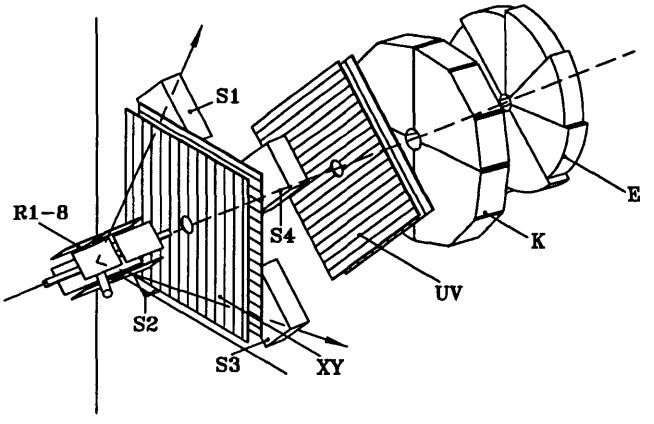

Figure 1. Perspective view of the A-region detectors, target cell in foreground. See text for a description of the detectors.

Scattered protons in the angular range $60° \leq \theta_{cm} \leq 120°$ were detected as coincidences between two opposite elements of the S1–S4 scintillators (25 cm × 25 cm × 5 cm). The hit position on the face of the detectors is determined from a position measurement by an XY wire chamber with a wire spacing of 3.2 mm (see Fig. 2). From the wire chamber information the difference $\delta\phi$ between the azimuthal angles of the two protons is determined

for each coincidence. The condition $\delta\phi=\pi$ has to be fulfilled for elastic scattering events. Figure 3 shows the $\delta\phi$ distribution at 450 MeV. Clearly, there is less than 1% background under the elastic peak. The background is believed to be caused by (p,2p) reactions in material along the beam other than the gas (presumably the walls of the target cell).

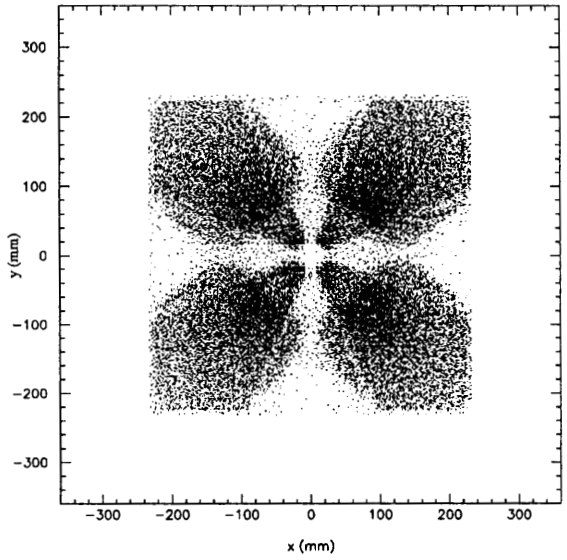

Figure 2. Hit pattern at the XY−chamber. Shown are the coordinates of coincidences between two opposite elements of the S1−S4 scintillators and coincidences between the K− or E−scintillator and one of the silicon detectors. The support structure of the end cap of the chamber causes the shadows.

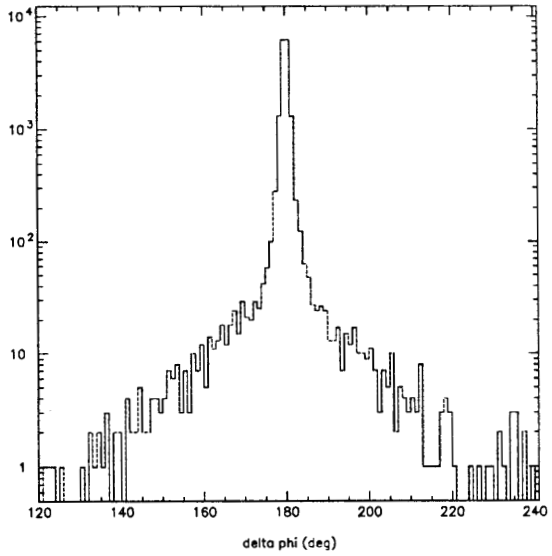

Figure 3. The difference of the azimuthal angles $\delta\phi$ of the two protons. Elastic scattering events are coplanar with $\delta\phi$=180°.

Data below θ_{cm}=70° were taken with the upgraded CE35 detector. Coincidences between the forward, segmented E−detector (E) or the segmented K−detector (K) and one of the eight position-sensitive silicon detectors R1−8 mounted alongside the target cell make a measurement at small angles (down to ~6° in the center of mass) possible. A new

set of silicon detectors was purchased for CE42. The detectors are equipped with a guard ring to remedy breakdown effects which were observed in the first set. In contrast to the original set of recoil detectors, the new detectors could be fully depleted. This was crucial for detection of some of the recoil protons at the highest energy (450 MeV) which are not stopped in the silicon detectors.

The events have no wire-chamber information at angles below 6° in the laboratory. In this case the forward-going proton passes through the central hole of *both* wire chambers *and* the K−scintillator before it is detected by the E−scintillator further downstream. The scattering angle for these events is calculated from the calibrated energy of the recoiling proton that is stopped in one of the silicon detectors. The silicon detectors are calibrated by eight permanently installed ^{241}Am sources. During the experiment the coincidence with the forward detector is disabled for dedicated runs to acquire silicon singles data in order to monitor the energy calibration. It has been shown that the calibration stays constant within 0.1% throughout a run. Fig. 4 shows the pp scattering cross section for events without wire chamber information as a function of laboratory scattering angle. The data have been normalized by an arbitrary factor. The rise in event rate due to Coulomb scattering at small angles is clearly visible.

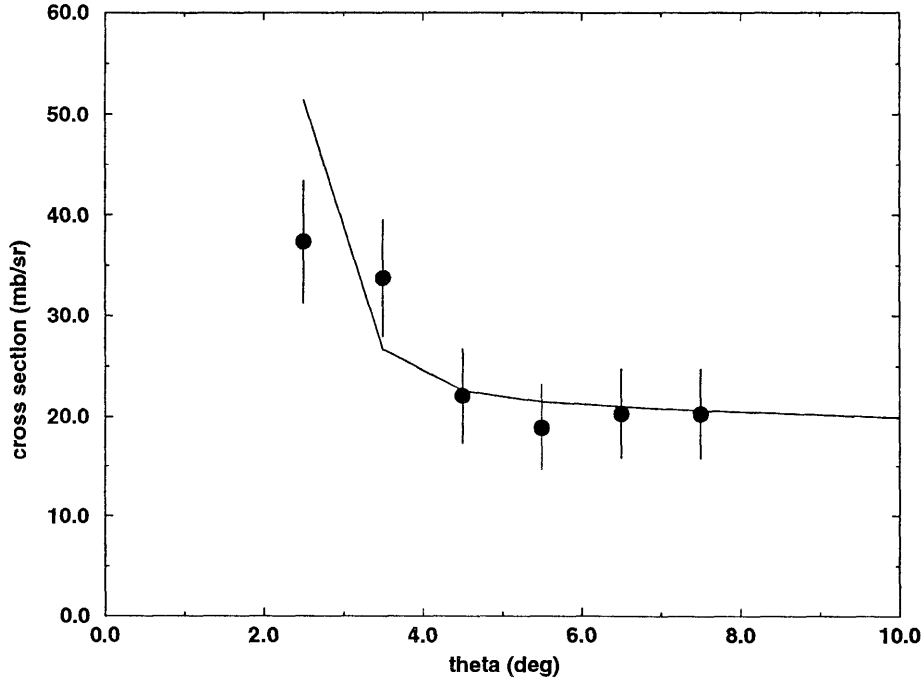

Figure 4. Cross section of pp elastic scattering as a function of laboratory angle at 400 MeV. The curve is the C400 solution from SAID. The data have been normalized with an arbitrary factor.

The experiment made use of up and down ramping the beam in the Cooler.[4] The experiment benefits in two ways from decelerated beam. First, if the beam polarization is known absolutely at the injection energy, the analyzing power at the high energy can be

calibrated. Second, the luminosity is increased since beam remaining at the end of a cycle is not discarded prior to injection for the next cycle.

In order to calibrate the analyzing power at the high energy, data were first taken at injection energy (200 MeV), then the beam was accelerated and data were taken with the same beam on the high energy flattop. Then the beam was decelerated to injection energy where another measurement, again with the same beam, was performed at 200 MeV. Since the analyzing power near 200 MeV is known absolutely,[5] beam and target polarization can be determined at injection energy. With the beam and target polarizations known, the analyzing power at the higher energy can be normalized.

The beam was not discarded at the end of each Cooler cycle but replenished with fresh beam from the cyclotron. The beam current in this mode ranged from 400 to 500 μA throughout the experiment. A typical cycle is shown in Fig. 5. At the beginning of each cycle the polarization direction of the stored beam was reversed using the spin–flipper[6] in order to reduce systematic uncertainties. The polarization of the injected beam was reversed every cycle at the ion source in order to replenish the ring with beam of the same polarization orientation as was stored in the ring.

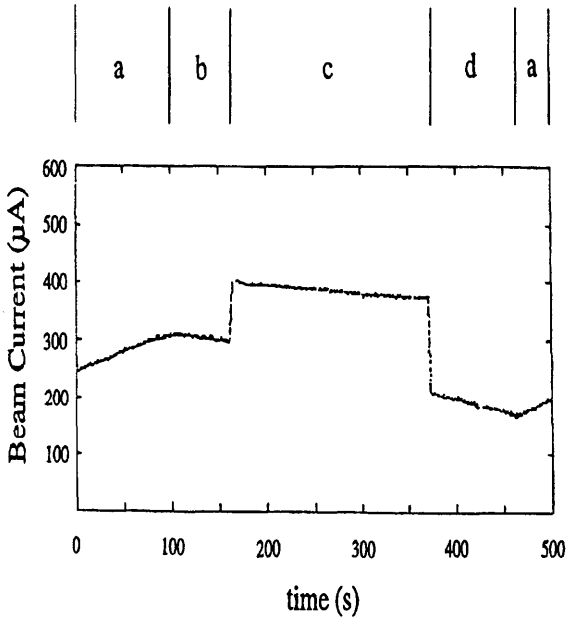

Figure 5. Beam current versus cycle time during an accel/decel cycle. The data are from CE-42, January 1996. Shown are the following phases: a) injection, b) data-taking at 200 MeV, c) data-taking at 400 MeV, d) data-taking at 200 MeV.

During one week of running, angular distributions of A_{xx}, A_{yy} and A_{xz} at angles between θ_{cm}=6° and θ_{cm}=90° were measured at eight energies (200, 250, 280, 295, 310, 350, 400 and 450 MeV). The data are now being analyzed. A statistical error of $\pm$0.02 per 1° bin in θ is expected for the spin correlation coefficients. The data at 200 MeV represent a remeasurement of CE35 augmented by additional angles.

The study of spin correlation coefficients in pp elastic scattering will continue with a measurement of A_{zz} at 200 MeV (CE45). This is expected to conclude the program of pp elastic scattering experiments with the polarized target in the A–region, which was in part motivated by the development of new capabilities for beam and target polarization

in a storage ring. Future uses of this facility include a study of pion production as well as three–body breakup in the d+p system.

1. T. Wise, A.D. Roberts, and W. Haeberli, Nucl. Instrum. and Methods **A336**, 410 (1993).
2. W.A. Dezarn, J. Doskow, J.G. Hardie, H.O. Meyer, R.E. Pollock, B. von Przewoski, T. Rinckel, F. Sperisen, W. Haeberli, B. Lorentz, F. Rathmann, M.A. Ross, T. Wise, P.V. Pancella, contrib. to *Eighth Int. Symp. on Pol. Phen. in Nucl. Phys.*, p. 62.
3. M.A. Ross, A.D. Roberts, T. Wise, W. Haeberli, W.A. Dezarn, J. Doskow, H.O. Meyer, R.E. Pollock, B. von Przewoski, T. Rinckel, F. Sperisen, and P.V. Pancella, Nucl. Instrum. and Methods **A344,** 307 (1994).
4. R.E. Pollock, see elsewhere in this report.
5. B. von Przewoski, H.O. Meyer, P.V. Pancella, S.F. Pate, R.E. Pollock, T. Rinckel, F. Sperisen, J. Sowinski, W. Haeberli, W.K. Pitts, and S. Price, Phys. Rev. C**44,** 44 (1991).
6. B. von Przewoski, W.A. Dezarn, J. Doskow, J.G. Hardie, H.O. Meyer, R.E. Pollock, T. Rinckel, F. Sperisen, W. Haeberli, B. Lorentz, F. Rathmann, M.A. Ross, T. Wise, and P.V. Pancella, Rev. Sci. Instrum. **1**, 67 (1996).

NEAR THRESHOLD PION PRODUCTION VIA ^{2}H($\vec{p}$,π^0)^{3}He

A. Betker, J. Cameron, W. Jacobs, H. Nann, T. Peterson,
J. Shao, M. Spraker, J. Szymanski, S. Vigdor, and K. Warman
Indiana University Cyclotron Facility, Bloomington, Indiana 47408

W.K. Pitts
University of Louisville, Louisville, Kentucky 40292

Reactions of the class (N,π) have generated renewed interest because the high momentum transfer (necessary to knockout a virtual pion) selects short range aspects of the NN interaction. Furthermore, it is expected that close to the pion-production threshold these reactions proceed in a non-resonant mode; that is, a real intermediate $\Delta(1232)$ which subsequently decays into a nucleon and a pion is not produced. Two previous experiments have examined the reaction ^{2}H(p,π^0)^{3}He near threshold. One of these was performed at IUCF[1] and the other at Saclay.[2] The results from these experiments show important discrepancies. The general trend of cross section σ versus $\eta \equiv p_{cm}/m_\pi$ is linear for the Saclay data but has a downward concavity for the IUCF data. Thus, the values of σ are not in agreement (in general) for a given η. The largest difference in the value of σ is for the highest η of the IUCF data set, $\eta = 0.20$:

IUCF Measurement	2.37 ± 0.07 μb,
Saclay Measurement	3.20 ± 0.04 μb.